Uncertainty in Scatterometer-Derived Vorticity

MARK A. BOURASSA AND KELLY MCBETH FORD

Department of Meteorology, and Center for Ocean-Atmospheric Prediction Studies, The Florida State University, Tallahassee, Florida

(Manuscript received 13 January 2009, in final form 2 September 2009)

ABSTRACT

A more versatile and robust technique is developed for determining area-averaged surface vorticity based on vector winds from swaths of remotely sensed wind vectors. This technique could also be applied to determine the curl of stress, and it could be applied to any gridded dataset of winds or stresses. The technique is discussed in detail and compared to two previous studies that focused on early development of tropical systems. Error characteristics of the technique are examined in detail. Specifically, three independent sources of error are explored: random observational error, truncation error, and representation error. Observational errors are due to random errors in the wind observations and determined as a worst-case estimate as a function of averaging spatial scale. The observational uncertainty in the Quick Scatterometer (QuikSCAT)-derived vorticity averaged for a roughly circular shape with a 100-km diameter, expressed as one standard deviation, is approximately 0.5×10^{-5} s^{-1} for the methodology described herein. Truncation error is associated with the assumption of linear changes between wind vectors. Uncertainty related to truncation has more spatial organization in QuikSCAT data than observational uncertainty. On 25- and 50-km scales, the truncation errors are very large. The third type of error, representation error, is due to the size of the area being averaged compared to values with 25-km length scales. This type of error is analogous to oversmoothing. Tropical and subtropical low pressure systems from three months of QuikSCAT observations are used to examine truncation and representation errors. Representation error results in a bias of approximately -1.5×10^{-5} s^{-1} for area-averaged vorticity calculated on a 100-km scale compared to vorticity calculated on a 25-km scale. The discussion of these errors will benefit future projects of this nature as well as future satellite missions.

1. Introduction

There are many oceanographic and meteorological applications for spatial derivatives of surface winds or surface stress. For example, Ekman upwelling in the ocean is related to the curl of the stress, and vertical motion in the atmosphere is related to the divergence. The calculation of divergence is noisy relative to the curl. The introduction of the Quick Scatterometer (QuikSCAT) SeaWinds instrument, launched on 19 June 1999, greatly improved data coverage and availability of ocean surface winds. These new data facilitated many studies, including research into the potential for earlier identification of tropical disturbances, which are possible precursors to tropical depressions (Katsaros et al. 2001; Sharp et al. 2002; Gierach et al. 2007). These studies suggested substantial noise in estimations of closed circulations and in the calculation of area-averaged vorticity. This study focuses on the calculation of the curl of wind from scatterometer swaths and the error characteristics as a function of spatial scale.

Sharp et al. (2002) developed an objective technique that could potentially be used operationally to identify systems (depressions and disturbances) likely to develop into tropical storms (TS) or hurricanes. Gierach et al. (2007) modified the method developed by Sharp et al. (2002) and applied it in conjunction with Geostationary Operational Environmental Satellite (GOES) IR to track tropical disturbances much further back in time than aforementioned methods. They found that convection and surface rotation were both found at the earliest identifiable stages of genesis. A critical component of these studies is the use of near-surface winds to examine circulation or rotation.

The main goals of this project are to improve upon the scatterometer-based calculation of area-averaged vorticity (referred to here simply as vorticity) and to characterize errors in this technique. The major sources of

Corresponding author address: Mark A. Bourassa, COAPS, The Florida State University, Tallahassee, FL 32306-2840.
E-mail: bourassa@coaps.fsu.edu

DOI: 10.1175/2009JTECHO689.1

error in the calculation of scatterometer-based surface vorticity are investigated and discussed. The strengths and weaknesses of the new and old methods (which focused on tropical systems) are discussed in terms of the improvements made upon earlier methods as well as considerations of how accuracy might change for prospective satellite missions.

The QuikSCAT SeaWinds data are described in section 2. Details regarding the methodology of the satellite-based vorticity calculation and comparisons to previous techniques are highlighted in section 3. Sources of error including ambiguity selection errors, random vector component errors, truncation errors, and representation errors are discussed in section 4. Section 5 covers opportunities for improvement for future applications. Overall, the detection technique continues to prove successful while reducing error in the results.

2. SeaWinds data

The QuikSCAT SeaWinds Scatterometer dataset used in this study is an updated version similar to that used by Gierach et al. (2007): version 3a of the Ku2001 product developed by Remote Sensing Systems (RSS). The dataset includes time, location, surface (10-m elevation) equivalent neutral wind speed (Ross et al. 1985), wind direction, and a rain flag. Scatterometers usually provide multiple solutions (termed ambiguities); only the best guess at the correct ambiguity is used for each wind vector cell. Four satellite microwave radiometers are used to determine if rain is present at the location of the QuikSCAT observation; when no radiometer data are available, the occurrence of adverse influences from rain is statistically estimated from the scatterometer backscatter (Mears et al. 2000a,b). This usage of the rain-flagging information is highly conservative. For tropical applications, a conservative rain flag appears to be necessary; however, this approach seriously overflags for midlatitude applications (Draper and Long 2004). The version of 25-km grid-spaced QuikSCAT data from the Jet Propulsion Laboratory (JPL) based on the QSCAT1 model function is also used to help quantify error characteristics.

A limitation for studies of tropical development is the temporal sampling, which has slightly less than twice daily coverage over the Atlantic basin (Schlax et al. 2001). In contrast, sampling is much better near the ice caps; however, cyclones tend to propagate very rapidly in these regions. Another key limitation for the calculation of surface vorticity is the spatial grid. The research-quality QuikSCAT observations used herein have a 25-km grid spacing within a swath that is 1800 km wide (76 vector wind cells across the swath). Therefore, the smallest spatial scale for which vorticity can be calculated is 25 km $\times$ 25 km, assuming that the spatial resolution of QuikSCAT observations is approximately a point. The actual scatterometer wind cell resolution depends on the processing technique used to convert the observed backscatter to wind vectors; however, it is smaller than the grid spacing (Bourassa et al. 2003). One other limiting factor is degradation of the accuracy of the wind vectors when too large a fraction of the signal returned to the satellite is due to rain (Draper and Long 2004; Weissman et al. 2002, 2003). The vorticity signatures of tropical systems are often associated with rain; therefore, it is important to develop a technique that is either insensitive to seriously rain-contaminated data or (in this case) attempts to avoid using such data.

The domain for this study is the portion of the Atlantic basin from the western coast of Africa to the east coast of North America and the equator to 30°N. Utilizing this area of the basin allows for most Atlantic tropical systems to be detected as well as limiting interference with midlatitude storm systems. This method for determining vorticity can be applied to any basin; however, the detection thresholds for tropical disturbances determined by Gierach et al. (2007) might require some modification.

3. Methodologies

Section 3a describes the technique used to calculate vorticity at a range of spatial scales. Section 3b puts this technique in the context of previous techniques used to identify tropical systems. The smoothing required for this approach is much different than required for two previous techniques, which are described in section 3b.

a. Vorticity calculation

Working with QuikSCAT swath data poses several issues in attempting an area-averaged vorticity calculation. Swaths are not in a perfectly gridded format, and some data points might be missing (because of land contamination or being outside the observational swath) or rain contaminated. To account for this, the calculation technique is developed to work around such points, and it outputs a missing value if there are insufficient good data points.

Area-averaged vorticity ζ is calculated at the center of a "shape," as defined by available data in the swath, using the circulation C about the shape and divided by the area A of the shape:

$$\zeta = \frac{C}{A}. \tag{1}$$

The circulation theorem is used to calculate the circulation:

$$C = \oint \boldsymbol{v} \cdot d\boldsymbol{l}, \tag{2}$$

where $\boldsymbol{v}$ is the velocity along the closed contour and $\boldsymbol{l}$ is an element tangent to the contour. The wind vector components are linearly interpolated between adjacent good observations: the shape about which the circulation is calculated becomes a series of straight segments. Then, $\int \boldsymbol{v} \cdot d\boldsymbol{l}$ becomes $\sum_{i=1}^{n} \boldsymbol{v}_i \cdot \boldsymbol{l}_i$, where i represents the segments from one to n. An individual dot product in this sum can be calculated as

$$\boldsymbol{v} \cdot \boldsymbol{l} = \frac{1}{2}(u_{i+1} + u_i, v_{i+1} + v_i)(x_{i+1} - x_i, y_{i+1} - y_i), \tag{3}$$

where x and y refer to the longitudinal and latitudinal positions (with differences in meters) and u and v are the zonal and meridional components of the surface wind vector. The circulation is the sum of (3), spanning the circumference of the shape.

If the shape is based on only three wind observations, the area (a triangle) is calculated using

$$A = 0.5[(x_2 - x_1)(y_3 - y_1) - (x_3 - x_1)(y_2 - y_1)]. \tag{4}$$

If four or more points are available, area and vorticity are calculated for a polygon using

$$A = 0.5\left|A_0 + \sum_{m=2}^{n-1} x_m(y_{m+1} - y_{m-1})\right| \quad \text{and} \tag{5}$$

$$A_0 = x_1(y_2 - y_1) + x_1(y_1 - y_n), \tag{6}$$

where n is the total number of points enclosing the polygon and the values of x and y are determined relative to the ''center of mass'' of the points used in the calculation.

Roughly circular shapes are used in this study; however, the shape about which the circulation is calculated is arbitrary and could be chosen to be consistent with the data and the application. The shapes used here are designed to have ''diameters'' that are multiples of the distance between adjacent observations. We refer to the size of these shapes as ''ring size.'' For 25-km grid-spaced QuikSCAT observations, a ring size of one corresponds to a 25-km-diameter square, a ring size of two corresponds to a 50-km-diameter diamond, and larger shapes become progressively more circular (see Fig. 1). The vorticity is then determined using the circulation from Eq. (3) and the area from Eqs. (4)–(6). If more than 20% of the vectors on the circumference of the shape are missing (or more than 25% when only four points are considered), the vorticity is also set to missing. If the threshold for too many missing points is not exceeded and there are missing points (e.g., land or seriously rain contaminated) in the ring perimeter, then there will be an atypically long line segment joining the neighboring points.

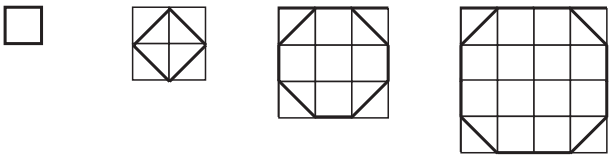

FIG. 1. Illustration of a ring size of 1–4 on a roughly 25 km × 25 km QuikSCAT observation grid. The bold lines show the perimeter of the ring.

b. Application to tropical disturbances

The tropical disturbance detection methods related to the surface signature (Sharp et al. 2002; Gierach et al. 2007) are vorticity based, with the relative area-averaged vorticity calculated within the QuikSCAT swath. Sharp et al. (2002) developed an objective technique that could potentially be used operationally to detect storm systems, in the topical disturbance or tropical depression stage of development, that were likely to develop to TS status or higher. The accuracy of this technique and the satellite sampling were less than ideal for independent operational use; therefore, it was suggested that this technique could supplement traditional techniques. Gierach et al. (2007) adapted the method developed by Sharp et al. (2002) and coupled it with GOES IR to track storms during the tropical disturbance stage of development. The technique used by Gierach et al. (2007) averages vorticity within SeaWinds swaths in a 100 km × 100 km area. Area-averaged vorticity values are calculated using the same technique developed by Sharp et al. (2002). For these detection techniques, the vorticity point was estimated over an area [7 × 7 wind cells for Sharp et al. (2002); 4 × 4 wind cells for Gierach et al. (2007)] and a test with four components is conducted:

1) The vorticity must exceed a minimum threshold:
   (i) 5×10^{-5} s^{-1} for Sharp et al. (2002) or
   (ii) 5×10^{-5} s^{-1} for Gierach et al. (2007).
2) The maximum non-rain-flagged wind speed within and on the periphery of the ring must exceed
   (i) 10.0 m s^{-1} for Sharp et al. (2002) or
   (ii) 6.3 m s^{-1} for Gierach et al. (2007).
3) The previous criteria must be met for at least a specified fraction of the vorticity points within an area with a diameter equal to the diameter used to calculate the vorticity. The area must be centered on the center of

mass of the observations used in the vorticity calculation. Typically, this area is equivalent to the points on and within the shape used to calculate the vorticity:
(i) 25 times within a 350 km by 350 km area centered on the center of circulation (Sharp et al. 2002) or
(ii) 80% of the calculated vorticity cells within 50 km of the vorticity points being tested.

4) Gierach et al. (2007) also required that the third condition must be met within 175 km of the center of a cloud cluster center determined from GOES IR.

The third point is important for reducing false alarms associated with questionable wind vectors: for example, vectors that perhaps should have been flagged as seriously rain contaminated or vectors with large directional errors. After it is determined where the first two criteria are met, the third criterion is examined at these locations and all locations within two grid points. Another factor that influences the vorticity's signal-to-noise ratio is the spatial scale over which vorticity is calculated. A larger spatial scale improves the identification of systems that are too rain contaminated: for example, tropical disturbances nearing the tropical depression stage or centers of stronger systems. For both these applications, the impact of errors (biases and random errors) is important to consider; however, the error characteristics of vorticity were not known when these techniques were developed.

A serious problem with this technique is that circulation about missing points in the interior also contributed to the estimate of circulation. Consequently, even seriously rain-contaminated vectors were used in the vorticity calculation in an attempt to eliminate rain contamination as a cause of missing vectors. The center of circulation of the systems detected could be no closer to the edge of a swath or a landmass than 150 km. Sharp et al. (2002) determined that this method of detection proved to be successful for both the 1999 and 2000 hurricane seasons and concluded that future operational use might prove beneficial when used in conjunction with traditional methods. Our new technique, applied with a diameter of 175 km, would likely be a more robust calculation, because neither interior circulations nor rain-flagged vectors contribute to the total, and the land constraint can be dropped.

4. Discussion of error

The important sources of error in our methodology stem from 1) observational errors, 2) truncation errors associated with linear interpolation between wind vectors, and 3) mismatches in the spatial averaging scale. It will be shown that the random errors in the area-averaged vorticity decrease as the ring size increases, but the rate of reduction is relatively small for ring sizes greater than 4 (a diameter of 100 km). Truncation error has a similar dependence on averaging scale; however. it has more organization within the QuikSCAT swath. Finally, the biases and standard deviations for differences in vorticity, for ring sizes 2–10 relative to a ring size of 1, are shown for Atlantic tropical disturbances and depressions.

a. Contributions from observational errors

Observational errors are due to (i) random vector component errors and (ii) ambiguity selection errors. Random errors for SeaWinds on QuikSCAT have been assessed through a variety of approaches (Freilich 1997; Stoffelen 1998; Ebuchi et al. 2002; Bourassa et al. 2003; Freilich and Vanhoff 2003, 2006). These studies typically investigate the random error where there was no gross error in direction related to ambiguity selection.

1) RANDOM ERRORS IGNORING AMBIGUITY SELECTION

The propagation of Gaussian-distributed random errors can be used to estimate the contribution of observational errors to uncertainty (expressed as a standard deviation) in area-averaged vorticity. For a variable y that is a function f of one or more independent variables x_i, this function can be described in very general terms as

$$y = f(x_1, x_2, x_3 \ldots). \tag{7}$$

The uncertainty in variable y, σ_y, can be determined [Eq. (8)] in terms of the uncertainty in the independent input variables x_i, again expressed as standard deviations (Taylor 1982):

$$\sigma_y^2 = \left(\frac{\sigma_{x_1}\partial f}{\partial x_1}\right)^2 + \left(\frac{\sigma_{x_2}\partial f}{\partial x_2}\right)^2 + \cdots. \tag{8}$$

This general formula for the propagation of independent random errors is the basis for Eqs. (9), (10), and (16). Assuming the area A is determined with negligible error (in a percentage sense), as is the random error in distance ℓ between the center of footprints, the uncertainty in the vorticity σ_ζ can be calculated as

$$\sigma_\zeta^2 = \frac{\sigma_C^2}{A^2}. \tag{9}$$

Examination of the area-calculated swaths through tropical and midlatitude storms indicate that the variability in area is very small, which supports the assumption that error in the area calculation can be ignored.

The uncertainty in circulation σ_c is

$$\sigma_C^2 = \sum_{i=1}^{n} (l_i \sigma_i)^2, \tag{10}$$

where σ_u is the uncertainty in a vector wind component, which is assumed to be 0.6 m s^{-1}. Estimates of random component errors for rain-free, correctly selected ambiguities, may be as large as 0.6 m s^{-1} for JPL's 25-km grid-spaced QuikSCAT data (M. H. Freilich and B. Vanhoff 2000, personal communication) for maximum differences in collocation of 30 min and 25 km. Estimates may plausibly be as low as 0.03 m s^{-1} (Bourassa et al. 2003) for RSS's dataset and collocation differences less than 0.5 min and 5 km. Assuming the highest error in vector components provides an upper limit for uncertainty in the vorticity and therefore represents a worst-case scenario. Furthermore, the accuracy is not uniform across the swath; however, because the chosen value includes uncertainty in the comparison data and differences resulting from mismatches in location and time, it is treated as a constant upper limit:

$$\sigma_C^2 = \sigma_u^2 \sum_{i=1}^{n} l_i^2. \tag{11}$$

Consequently,

$$\sigma_C^2 = \sigma_u^2 (n_1 + 2n_2) l^2, \tag{12}$$

where n_1 and n_2 represent the number of ''nondiagonal'' and ''diagonal'' components of the area perimeter, respectively (Fig. 1). The length of the diagonal components is $\sqrt{2}$ times the distance (Δx) between the across-swath or along-swath cells (which is close to constant). The observational uncertainty in vorticity σ_{ζ_O} is defined as follows:

$$\sigma_{\zeta_O} = \sigma_u (n_1 + 2n_2)^{0.5} \frac{l}{A} \tag{13}$$

The area increases more rapidly than the number of points on the perimeter of the area; therefore, σ_{ζ_O} decreases as area increases (Fig. 2).

The uncertainty can also be expressed in terms of diameter and the grid spacing, which might make the application more intuitive, particularly when considered for non-QuikSCAT applications. Consider that the number of points on the perimeter times the grid spacing is roughly equal to the length of the perimeter, which is proportional to the diameter. The area is proportional to the diameter squared:

$$\sigma_{\zeta_O} \approx 4\pi^{-0.5} \sigma_u D^{-1.5} \Delta x^{0.5}. \tag{14}$$

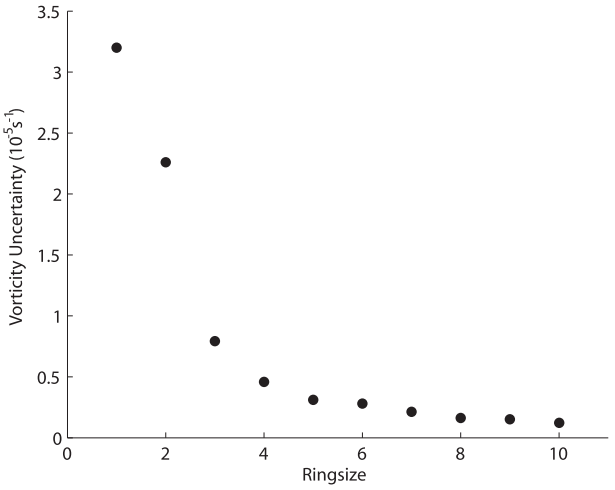

FIG. 2. Vorticity uncertainty (representing 1 std dev) as a function of ring size. The studies by Sharp et al. (2002) and Gierach et al. (2007) used a ring size of 1 with a great deal of additional smoothing.

This analysis shows that, as ring size increases, vorticity uncertainty (Fig. 2) is proportional to $D^{-1.5}$. For diameters exceeding four grid cells, the decrease in uncertainty is small. Therefore, choosing a ring size larger than 4 would result in only slightly lower levels of uncertainty, and it would negatively affect the detection technique's ability to maintain the integrity of smaller-scale systems because of representation error (section 4c).

2) AMBIGUITY SELECTION ERROR

Ambiguity selection errors are errors associated with selecting the wrong local minimum in the best fit of a wind vector to observed backscatter (Naderi et al. 1991; Bourassa et al. 2003). The likelihood of an ambiguity selection error is a function of wind speed: it is highly unlikely for wind speeds greater than 8 m s^{-1} (for the RSS product) and increases as the wind speed decreases below 8 m s^{-1}. This model of error suggests that the standard deviation of errors in vorticity might be relatively large for low wind speeds. However, it has also been argued that this dependency on wind speed can be largely explained in terms of random errors in wind vector components, where characterization of these random errors is not a function of wind speed (Freilich 1997). That model for observational errors in wind vectors results in vorticity error characteristics that are independent of wind speed.

If ambiguity errors make a substantial contribution to observational errors, then the observational error will increase as the wind speed decreases below 8 m s^{-1}. This dependency on wind speed is examined to determine if

there is a substantial contribution from ambiguity errors. The root-mean-square differences (RMSDs) of vorticity are calculated, where the difference is the vorticity at a ring size (from 1 to 9) minus the vorticity for ring size 10. A ring size 10 has a larger spatial area (diameter of 250 km), which reduces the influence of ambiguity errors in the vorticity calculation. Atlantic tropical disturbances (from 5° to 35°N) from 1 August through 31 October 1999 were used to examine the importance of considering additional errors associated with ambiguity selection. For each ring size, the scalar mean wind speed is determined from the wind vectors used in the vorticity calculation. These mean speeds are binned in increments of 1 m s^{-1} (from 0 to 20 m s^{-1}), and the values in these bins are used to calculate the RMSDs. There is no evidence of a wind speed dependency. This indicates that ambiguity selection errors are typically a weak source of observational error in the vorticity or that observational error is negligible compared to truncation error (as will be shown to be the case in the next section).

b. Truncation error

The term "ring" is used somewhat loosely, because wind vector spacing only allows a roughly circular shape (Fig. 1) composed of a series of straight edges. An assumption is made that the wind speeds change linearly along the segments of the ring. The error in this assumption is related to higher-order changes and the grid spacing. The actual changes of wind speed along the segment can be substantially nonlinear: for example, centers of strong low pressure systems and poorly organized tropical disturbances. The shape of tropical disturbances varies greatly system by system as well as in time. If some points in the ring perimeter are considered bad points (e.g., land or seriously rain contaminated), then there will be an atypically long line segment joining the neighboring points. This situation can greatly increase truncation errors associated with the linear extrapolation of wind speeds.

Assuming that the truncation errors are random and approximately similarly distributed for each segment along the edges of the shape (i.e., triangle, square, or polygon), the total variance associated with random errors in the circulation around the shape σ_C^2 is approximately proportional to the number of segments times the square of the truncation error uncertainty squared σ_T^2 of each segment. The number of segments is approximated as the number of points ($\pi D/\Delta x$) for a perimeter of a circle associated with a diameter D:

$$\sigma_C^2 = \sigma_T^2 \frac{\pi D}{\Delta x}. \tag{15}$$

Error associated with the area calculation is again ignored. The assumption of totally random truncation errors is not entirely sound, because the wind field is made up of a larger-scale (organized) flow and smaller-scale (seemingly random) departures from this flow. For regularly gridded data and large-scale variability that greatly outweighs small-scale variability, the projection of the truncation error onto a particular line segment (in the ring) will slowly change in space. Such a situation results in large-scale errors that nearly cancel on the opposite side of the ring. In this case, it might be more appropriate to treat the differences in these nearly cancelling truncation errors as independent, effectively halving the number of points in the error calculation. However, if the grid pattern is sufficiently nonuniform or if the small-scale variability is greater than the large-scale variability (which is not the case for cyclones), then the assumption of random errors is closer to being valid. The influence of the irregular spacing of QuikSCAT wind vectors will be shown to be important later in this section.

The uncertainty in vorticity σ_s associated with truncation errors is then, to a good approximation, equal to the related uncertainty in circulation divided by the area about which the circulation is calculated. Consequently, the uncertainty in vorticity related to truncation error σ_{s_T} has the following functional form:

$$\sigma_{s_T} \approx 4\pi^{-0.5} \sigma_T D^{-1.5} \Delta x^{0.5}. \tag{16}$$

The uncertainty in wind related to truncation error σ_T is roughly proportional to the square of the length of each segment, which is roughly proportional to $(\Delta x)^2$. Therefore, σ_{s_T} is proportional to $(\Delta x)^{2.5}$:

$$\sigma_{s_T} \propto D^{-1.5} \Delta x^{2.5}. \tag{17}$$

As one would anticipate, finer grid spacing will reduce truncation errors, as will increasing the diameter of calculation area. However, increasing the area results in a vorticity averaged over a larger area, which has shortcomings discussed in the next section.

If a truncation error is apparent in the QuikSCAT vorticity fields, it is because either the small-scale wind variability dominates the large-scale wind variability (which is not the case for the examples that will be shown) or the irregularity in the spatial sampling increases the impact of truncation errors. The vorticity fields are shown for two cases for ring sizes of 1–4 (25–100-km averaging scales). The first case is a strong warm core seclusion (Fig. 3, left) in the North Pacific Ocean from 24 December 2004. The second case is a tropical disturbance from 2000 UTC 4 September 1999 (Fig. 3, middle), which might

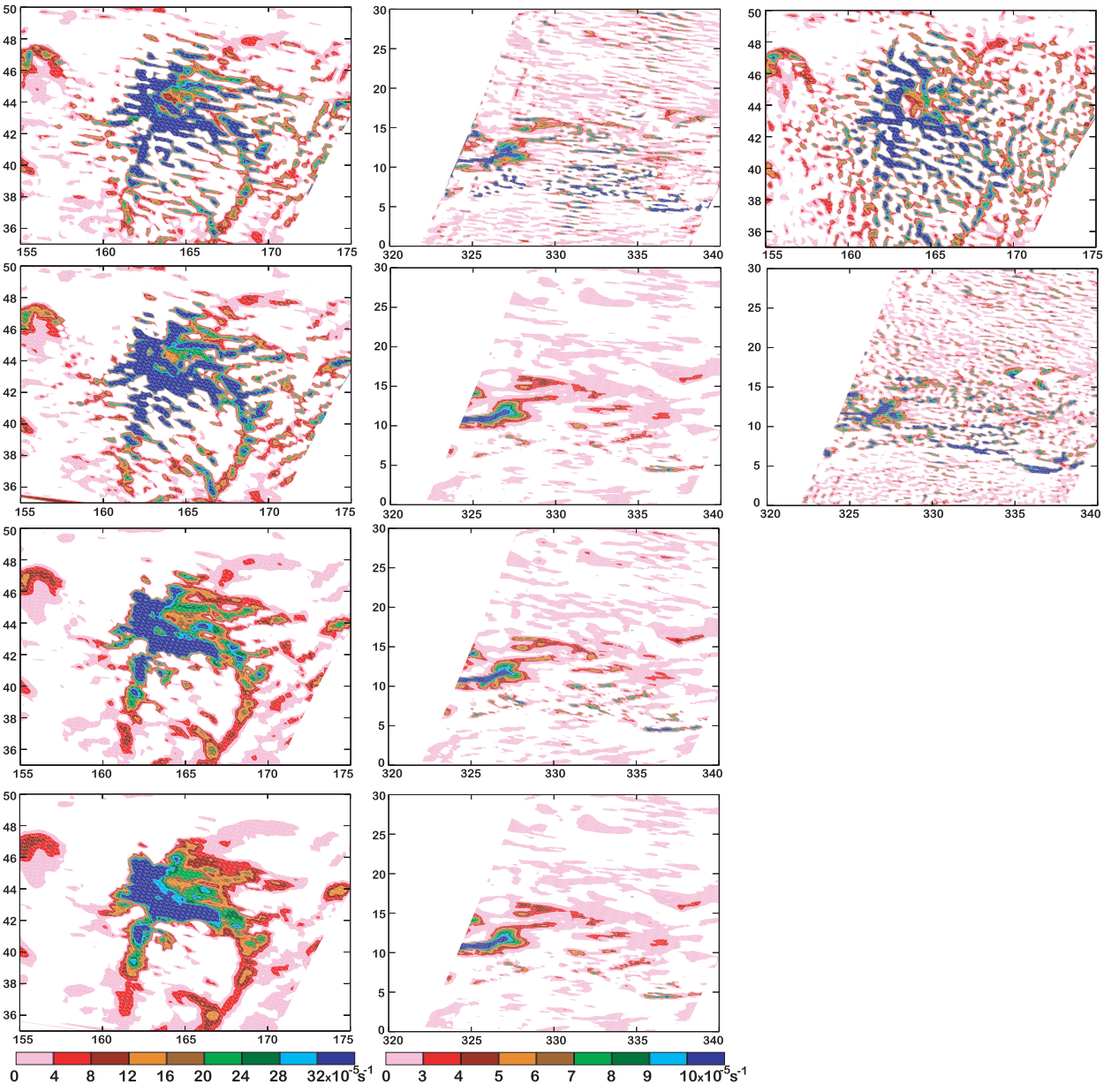

FIG. 3. Vorticity fields from two cases and ring sizes (top)–(bottom) 1–4: (left) strong warm core seclusion in the North Pacific Ocean (24 Dec 2004) and (middle) a tropical disturbance from 2000 UTC 4 Sep 1999 that might have contributed to Hurricane Floyd. The images are based on (left), (middle) RSS wind vector retrievals and (right) JPL's retrievals and a ring size of one; the JPL images correspond to (top left) and (top middle).

have contributed to Hurricane Floyd. In both 25-km cases (ring size 1), there is a strong across-swath pattern. This pattern diminishes in strength as the averaging diameter increases, and it is difficult to identify when the averaging scale reaches about 100 km. The left and middle of Fig. 3 are based on RSS's version of the 25-km grid-spaced QuikSCAT data, whereas Fig. 3, right, is based on JPL's product. Note that the random observation uncertainty in an earlier version of RSS's product was roughly 60% of the uncertainty in JPL's product, partly because of mild smoothing of the backscatter prior to the RSS retrievals. K. Hilburn (2008, personal communication) has shown that the vorticity pattern is very similar to the pattern of changes in the along-swath grid spacing, as was suggested by D. Long (2008, personal communication), which causes the largest asymmetry in the ring shape. This pattern is much harder to identify in the JPL-based images, suggesting that the influence of observational noise is closer

in magnitude to the truncation-related noise in JPL's products. Existing estimates of the observational noise include a substantial variance resulting from natural variability and mismatches in space and time (Bourassa et al. 2003); therefore, it is difficult provide a good estimate of the constant of proportionality in (17).

c. Representation error

Representation errors are due to approximating something as something else. For example, QuikSCAT winds correspond to certain spatial/temporal scales but are often validated through comparison to buoy winds, which have a much different spatial/temporal scale and are often centered at different times and locations. Each of these mismatches is a type of representation error. Representation errors can have both a bias and a random component. In the case of the vorticity calculation, spatial averaging errors are a factor when the wind vectors associated with an area-averaged vorticity maximum are within the ring used in the vorticity calculations. The larger the ring size, the more potential there is for a localized vorticity maximum to be missed. Strictly speaking, if the spatial scale used in the vorticity calculation is the desired scale, then there is no representation error. In the case of cyclonic systems, representing finer-scale vorticity with larger-scale vorticity results in random errors and a negative bias (an underestimation of positive vorticity).

Atlantic tropical and subtropical systems that meet the detection criteria for tropical disturbances, 488 overpasses of systems from 1 August through 31 October 1999, were examined to estimate the bias and random errors associated with representation errors. These are systems typical of our applications. The bias (Fig. 4) shows the change in vorticity relative to the vorticity for a ring size 1 (diameter of 25 km). For vorticity calculated with an odd number of grid cells in the diameter, the center of the larger area calculation is very close to that with a ring size of one. For vorticity calculated with an even number of grid cells in the diameter, the center of the larger area calculation is shifted roughly 17.6 km up the swath and to the right (half of a grid cell in both directions). This change in location contributes to the $2\Delta x$ wobble for large ring sizes in Fig. 4. The standard deviations are not shown, because they also include substantial contributions from truncation errors. The bias increases in magnitude as ring size increases, with a bias of approximately -1.5×10^{-5} s^{-1} for a ring size 4 (diameter of 100 km). The magnitude of the bias does not decrease much beyond a ring size 5; thus, choosing a ring size higher than 5 does little to increase the magnitude of the bias from this area assumption for this application. The bias typical of tropical disturbances and TSs (-1.5×10^{-5} s^{-1}) could impact on the application of finding tropical disturbances, because the detection threshold is slightly more than 3 times larger (5×10^{-5} s^{-1}) than the bias, however, and any bias was presumably factored into the threshold. Different biases will be typical of other types of weather (e.g., fronts or high pressure systems); therefore, the shown biases should not be assumed to apply to all situations.

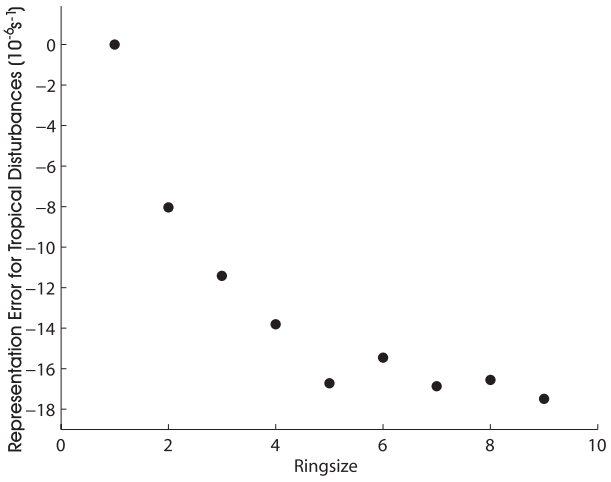

FIG. 4. Plot of mean differences for each ring size minus ring size 1, illustrating the biases resulting from representation (spatial averaging) areas associated with tropical and subtropical systems. As the ring size increases, the area over which the vorticity is averaged increases. This enlargement in area enhances the bias by smoothing the small-scale cyclonic features.

5. Opportunities for improvement and application

As indicated in section 4, errors in the SeaWinds dataset and approximations resulting from characteristics of the dataset (e.g., grid spacing) are important considerations when dealing with applications that are sensitive to these errors. Improvements in related satellite technology could do wonders for future applications of this technique. One of the greatest changes is improved temporal sampling resulting from multiple scatterometers in orbit [currently QuikSCAT and the Advanced Scatterometer (ASCAT), with the Indian scatterometer on *Oceansat-2* expected soon]. ASCAT's greatly reduced rain contamination (resulting from the use of C band rather than Ku band) is likely to be a substantial advantage; however, this is offset by reduced resolution (roughly 50 km) in the product with 25-km grid spacing.

Increased resolution and finer grid spacing (and reduced sensitivity to rain), such as is proposed in the Extended Ocean Vector Wind Mission (XOVWM), would allow for reductions in truncation error in comparison to calculation with a similar averaging diameter. Alternatively, this error could be reduced by making

a more uniform spatial sampling within the swath. The finer spatial resolution should also result in better estimates of random observational errors because of close collocations, which will also reduce our overestimation of the observational errors. Alternatively, the trial storm diameter could be reduced (without increasing noise) to provide significant decreases in biases (representation errors). The choice trade-off between reduced bias and reduced random errors would depend on the specifics of the application. For example, the application of forecasting transition to named storms (Sharp et al. 2002) has different requirements than the early detection of tropical disturbances (Gierach et al. 2007). The method developed by Sharp et al. (2002) might not benefit from smaller spatial scales, because this would increase random errors, whereas the reduction of noise in larger-scale estimates might make the forecasts more accurate.

6. Conclusions

The improved calculation of scatterometer-based area-averaged vorticity developed here can be used for tropical system detection, such as those demonstrated by Sharp et al. (2002) and Gierach et al. (2007), as well as studies of vorticity at other latitudes and from any gridded product. Improvements include a more accurate calculation of area, a better handling of missing data (resulting from serious rain-contamination flags, land, and swath edges), characterization of the key sources of error, and applicability to any gridded fields of winds or stresses. An understanding of the trade-offs between averaging area and noise should be useful for all vorticity-based applications. The spatial averaging scale of the vorticity calculation is very easily adjusted from the native grid spacing up to an arbitrarily large size within the observational swath. This versatility makes it easy for a spatial scale to be chosen to match the needs of the application or for a range of spatial scales to be considered. In the case of tropical disturbances, the range of spatial scales is highly useful for the identification of circulations when there is often a great deal of serious rain contamination to be avoided.

The error characteristics of the area-averaged vorticity calculation can be described in terms of three types of errors: random observational error, truncation error associated with linear interpolation between wind vectors, and mismatches in the spatial averaging scale (representation errors). The random observational error can be characterized in terms of an isotropic random vector error, with the number of observations defining the perimeter of the area and size of the area. This random error has a standard deviation that is approximately proportional to the random vector error, the diameter raised of the area raised to the -1.5 power and grid spacing to the 0.5 power. That is, larger areas decrease the random error and finer grid spacing along the perimeter increases the number of data points, which consequently increases the random error. Ambiguity selection errors are either adequately described by the random vector component errors or much smaller than truncation errors.

Truncation errors are based on the linear interpolation between grid points along the perimeter of the ring projected onto the line segments making up the ring. For a regular grid and a smooth large-scale flow, errors on one side of the ring will be approximately canceled by errors on the other side of the ring. QuikSCAT's slightly irregular sampling pattern makes these errors quite apparent in swaths of vorticity. This random error has a standard deviation that is approximately proportional to the diameter raised of the area raised to the -1.5 power and grid spacing to the 2.5 power. Truncation-related errors can be reduced by increasing the averaging area and by increasing the resolution of the wind vectors. Truncation errors will be the most severe where vectors have been dropped from the calculation because of serious rain contamination; therefore, an instrument that is less impacted by rain would be quite advantageous for many applications.

Representation errors result in a random error and a negative bias (underestimation of positive vorticity) when sampling cyclonic systems. This bias is substantial in comparison to the vorticity thresholds used in the Sharp et al. (2002) and Gierach et al. (2007) techniques. These thresholds are empirically chosen to match the spatial smoothing with the study's objective. In a more general sense, these three types of error should be considered in any study of satellite-based vorticity. When applied to a truly regularly gridded product, truncation errors associated with the curl, wind, or stress will be very small, except when there is a large change in the curvature of the wind field across the spatial scale used in the curl calculation. The truncation error is highly dependent on the variability in the satellite sampling pattern, and it is likely to be quite different from instrument to instrument. An instrument, such as the proposed XOVWM, with 5–25 times the resolution (in one dimension) would greatly reduce both the truncation and the representation errors.

Acknowledgments. Funding for this research was provided by the NASA Tropical Cloud Systems and Processes (TCSP) Experiment and the NASA Ocean Vector Wind Science Team. We thank Deborah Smith, Kyle Hilburn, David Long, Philip Cunningham, and Paul Reasor for their interactions.

REFERENCES

Bourassa, M. A., D. M. Legler, J. J. O'Brien, and S. R. Smith, 2003: SeaWinds validation with research vessels. *J. Geophys. Res.,* **108,** 3019, doi:10.1029/2001JC001028.

Draper, D. W., and D. G. Long, 2004: Simultaneous wind and rain retrieval using SeaWinds data. *IEEE Trans. Geosci. Remote Sens.,* **42,** 1411–1423.

Ebuchi, N., H. C. Graber, and M. J. Caruso, 2002: Evaluation of Wind vectors observed by QuikSCAT/SeaWinds using ocean buoy data. *J. Atmos. Oceanic Technol.,* **19,** 2049–2062.

Freilich, M. H., 1997: Validation of vector magnitude datasets: Effects of random component errors. *J. Atmos. Oceanic Technol.,* **14,** 695–703.

——, and B. A. Vanhoff, 2003: The relationship between winds, surface roughness, and radar backscatter at low incidence angles from TRMM precipitation radar measurements. *J. Atmos. Oceanic Technol.,* **20,** 549–562.

——, and ——, 2006: The accuracy of preliminary WindSat vector wind measurements: Comparisons with NDBC buoys and QuikSCAT. *IEEE Trans. Geosci. Remote Sens.,* **44,** 622–637, doi:10.1109/TGRS.2006.869928.

Gierach, M. M., M. A. Bourassa, P. Cunningham, J. J. O'Brien, and P. D. Reasor, 2007: Vorticity-based detection of tropical cyclogenesis. *J. Appl. Meteor. Climatol.,* **46,** 1214–1229.

Katsaros, K. B., E. B. Forde, P. Chang, and W. T. Liu, 2001: QuikSCAT's SeaWinds facilitates early identification of tropical depressions in 1999 hurricane season. *Geophys. Res. Lett.,* **28,** 1043–1046.

Mears, C. A., D. K. Smith, and F. J. Wentz, 2000a: Detecting rain with QuikScat. *Proc. IGARSS,* Honolulu, HI, IEEE, 1235–1237.

——, F. J. Wentz, and D. K. Smith, 2000b: SeaWinds on QuikSCAT normalized objective function rain flag. Remote Sensing Systems Product Description Version 1.2, 13 pp.

Naderi, F. M., M. H. Freilich, and D. G. Long, 1991: Space borne radar measurements of wind velocity over the ocean—An overview of the NSCAT scatterometer system. *Proc. IEEE,* **79,** 850–866.

Ross, D. B., V. J. Cardone, J. Overland, R. D. McPherson, W. J. Pierson Jr., and T. Yu, 1985: Oceanic surface winds. *Adv. Geophys.,* **27,** 101–138.

Schlax, M. G., D. B. Chelton, and M. H. Freilich, 2001: Sampling errors in wind fields constructed from single and tandem scatterometer datasets. *J. Atmos. Oceanic Technol.,* **18,** 1014–1036.

Sharp, R., M. A. Bourassa, and J. J. O'Brien, 2002: Early detection of tropical cyclones using SeaWinds-derived vorticity. *Bull. Amer. Meteor. Soc.,* **83,** 879–889.

Stoffelen, A., 1998: Toward the true near-surface wind speed: Error modeling and calibration using triple collocation. *J. Geophys. Res.,* **103,** 7755–7766.

Taylor, J. R., 1982: *An Introduction to Error Analysis: The Study of Uncertainties in Physical Measurements*. University Science Books, 270 pp.

Weissman, D., M. A. Bourassa, and J. Tongue, 2002: Effects of rain rate and magnitude on SeaWinds scatterometer wind speed errors. *J. Atmos. Oceanic Technol.,* **19,** 738–746.

——, ——, ——, and J. J. O'Brien, 2003: Calibrating the QuikSCAT/SeaWinds radar for measuring rain over water. *IEEE Trans. Geosci. Remote Sens.,* **42,** 2814–2820.